Solvation of Transition Metal Ions by Water. Sequential Binding Energies of $M^+(H_2O)_x$ (x = 1–4) for M = Ti to Cu Determined by Collision-Induced Dissociation

N. F. Dalleska, Kenji Honma,† L. S. Sunderlin,‡ and P. B. Armentrout*

Contribution from the Department of Chemistry, University of Utah, Salt Lake City, Utah 84112

Received October 15, 1993. Revised Manuscript Received January 3, 1994•

Abstract: Thresholds for collision-induced dissociation of $M^+(H_2O)_x$ (x = 1–4, M = Ti to Cu) with xenon are measured by using guided ion beam mass spectrometry. In all cases, the primary product is endothermic loss of one water molecule. The cross-section thresholds are interpreted to yield 0 K bond energies after accounting for the effects of multiple ion–molecule collisions, internal energy of the clusters, and dissociation lifetimes. Overall, the results presented here are consistent with previously reported values for x = 1 and 2 and resolve several discrepancies in these values. Theory is shown to accurately predict the BDEs of x = 1 and 2 as well as the sign of the difference between them. For all ions but Mn^+, the bond dissociation energies (BDEs) of the first and second water molecules are large compared with those of the third and fourth water molecules. Trends in BDEs are discussed in terms of hybridization and spin changes occurring at the transition metal center.

Introduction

Fundamental to understanding the solvation of ions is the interaction of individual ions with individual solvent molecules. Water is ubiquitous in both chemistry and life, and hence is a solvent of particular interest. One means of gaining insight into these complex, multicentered interactions is to measure the sequential bond dissociation energies (BDEs) of metal ions to successive solvent molecules. Such studies are an important way of bridging the gap between ion chemistry in the gas-phase and that in solution.

Dzidic and Kebarle[1] have performed thermal equilibrium measurements of alkali metal ion–water systems. They found that the BDEs in these systems decrease monotonically as the number of ligands increases and as the ionic radius of the metal increases. These trends are consistent with an electrostatic bonding mechanism in which two phenomena serve to reduce the bond energy as the number of ligands increases. One, the charge becomes increasingly delocalized, resulting in decreased ion–dipole and ion–induced dipole interactions. Two, the ligands begin to crowd one another, and the resulting ligand–ligand repulsion lowers the bond energy. Ultimately, the inner solvent shell is filled and additional ligands cannot bind directly to the metal ion. Ions with larger radii bind ligands less strongly because the ligands cannot approach the ion as closely.

Until recently, $Cu^+(H_2O)_x$ were the only first-row transition metal ion bound water clusters for which BDEs had been measured.[2,3] Holland and Castleman measured the BDEs of $Cu^+(H_2O)_x$ where x = 3–5 and found tha the BDEs decreased with increasing x, a trend similar to the alkali metal ion complexes. In contrast collision-induced dissociation (CID) measurements by Magnera et al.,[4] Magnera, David, and Michl (MDM),[5] and Marinelli and Squires (MS)[6] found that a second water ligand is bound to some first-row transition metal ions more strongly than the first. In general, results from these two groups agree qualitatively, although there are a couple of quantitative discrepancies. Ab initio calculations of Rosi and Bauschlicher (RB)[7] and Bauschlicher, Langhoff, and Partridge (BLP)[8] agree qualitatively with these experimental results for all but $Ni^+(H_2O)_x$, where theory predicts $Ni^+(H_2O)$ to be bound more strongly than $Ni^+(H_2O)_2$ in contrast to the experimental results.[5,6]

The two previous studies of the $M^+(H_2O)_x$ (x = 1 and 2) systems differ in several ways. In the studies by Michl and coworkers[4,5] ion bound clusters were produced by fast atom and ion bombardment of ice on or containing a transition metal. Cluster ions formed are then sampled directly into a triple quadrupole instrument equipped for CID studies in the central rf-only quadrupole. Clusters are cooled from their initially warm state only by the loss of water molecules via unimolecular decomposition. Cluster ions formed this way retain appreciable internal excitation as confirmed by MDM's observation that their cluster ion beams contain 1 to 10% metastable ions. To try to compensate for the unknown internal energy distribution, BDEs are obtained from the *differences* between primary and secondary thresholds and between successive secondary thresholds. MS[6] produced their cluster ions in a flowing afterglow apparatus where clusters are formed under thermal conditions. They produce ions of the general type $M(CO)_x^+$ by adding volatile metal carbonyl compounds to a flow containing excited helium atoms. The $M(CO)_x^+$ then undergo ligand exchange reactions with H_2O to form the cluster ion of interest. This ion source is similar to the one used in the present work, and the internal energy distribution is well-characterized. Primary thresholds are used to obtain BDEs, although MS analyze their data and treat the internal energy of the cluster differently than we do here, as discussed in detail below.

In this paper, we report the BDEs of water molecules to the first-row transition metal positive ions as determined by CID in a guided ion beam mass spectrometer. The CID results are carefully analyzed to account for a variety of systematic effects that would otherwise distort the thermochemistry obtained. BDEs

† Permanent address: Department of Material Science, Himeji Institute of Technology, Kamigori, Hyogo, Japan 678-12.
‡ Present address: Department of Chemistry, Purdue University, West Lafayette, Indiana 47904.
• Abstract published in *Advance ACS Abstracts*, March 15, 1994.
(1) Dzidic, I.; Kebarle, P. *J. Phys. Chem.* **1970**, *74*, 1466.
(2) Holland, P. M.; Castleman, A. W., Jr. *J. Am. Chem. Soc.* **1980**, *102*, 6174. Holland, P. M.; Castleman, A. W., Jr. *J. Chem. Phys.* **1982**, *76*, 4195.
(3) Burnier, R. C.; Carlin, T. J.; Reents, W. D., Jr.; Cody, R. B.; Lengel, R. K.; Freiser, B. S. *J. Am. Chem. Soc.* **1979**, *101*, 7127.
(4) Magnera, T. F.; David, D. E.; Stulik, D.; Orth, R. G.; Jonkman, H. T.; Michl, J. *J. Am. Chem. Soc.* **1989**, *111*, 5036.
(5) Magnera, T. F.; David, D. E.; Michl, J. *J. Am. Chem. Soc.* **1989**, *111*, 4100.
(6) Marinelli, P. J.; Squires, R. R. *J. Am. Chem. Soc.* **1989**, *111*, 4101.
(7) Rosi, M.; Bauschlicher, C. W., Jr. *J. Chem. Phys.* **1989**, *90*, 7264. Rosi, M.; Bauschlicher, C. W., Jr. *J. Chem. Phys.* **1990**, *92*, 1876.
(8) Bauschlicher, C. W., Jr.; Langhoff, S. R.; Partridge, H. *J. Chem. Phys.* **1991**, *94*, 2068.

0002-7863/94/1516-3519$04.50/0

for titanium through copper ions bound to between one and four water molecules are reported. These results are compared with the previous experimental and theoretical work for one and two water complexes. Results for three and four water complexes are the first available for all metals but vanadium and copper. The periodic trends in these values are discussed and analyzed in terms of the electronic configurations of these unsaturated clusters and simple ligand field ideas.

Experimental Section

General. Complete descriptions of the apparatus and experimental procedures are given elsewhere.[9,10] The production of metal ion bound water clusters is described below. Briefly, ions are extracted from the source, accelerated, and focused into a magnetic sector momentum analyzer for mass analysis. Mass-selected ions are slowed to a desired kinetic energy and focused into an octopole ion guide that radially traps the ions. The octopole passes through a static gas cell containing the xenon collision gas. After exiting the gas cell, product and unreacted beam ions drift to the end of the octopole where they are focused into a quadrupole mass filter for mass analysis and then detected. Ion intensities are converted to absolute cross sections as described previously.[9] Absolute uncertainties in cross section magnitudes are estimated to be ±20%, and relative uncertainties are ±5%.

Laboratory ion energies are related to center-of-mass (CM) frame energies by $E(\mathrm{CM}) = E(\mathrm{lab})m/(M + m)$ where M and m are the ion and neutral reactant masses, respectively. All energies cited below are in the CM frame unless otherwise noted. Sharp features in the observed cross sections are broadened by the thermal motion of the neutral gas and the distribution of ion energies. The full width at half maximum (fwhm) of the neutral gas motion at nominal energy, $E(\mathrm{CM})$, is given by fwhm $\approx [11.1\ k_B TEM/(M + m)]^{1/2}$.[11] The fwhm of the ion beam energy distribution was typically between 0.2 and 0.6 eV lab for these experiments. The zero of the absolute energy scale and the ion energy distribution are measured by a retarding potential technique described elsewhere.[9] The uncertainty in the absolute scale is ±0.05 eV lab, which corresponds to 0.03 eV CM for the lightest cluster studied, $Ti^+(H_2O)$, to 0.02 eV for the heaviest, $Cu^+(H_2O)_4$. Because the energy analysis region and the reaction zone are physically the same, ambiguities in the energy analysis resulting from contact potentials, space charge effects, and focusing aberrations are minimized. Experiments conducted at low kinetic energies are consistent with absolute kinetic energies accurate within the cited uncertainty.[12,13]

Ion Source. The cluster ions are formed in a 1 m long flow tube[10] operating at a pressure of 0.4–0.7 Torr with a helium flow rate of 4000–9000 standard cm^3/min. Three methods were used to produce cluster ions with typical intensities between 5×10^4 and 2×10^6 ions/s. In the first method, metal ions are generated in a continuous dc discharge by argon ion sputtering of a cathode fabricated from the metal of interest.[14] Clusters are formed by associative reactions with water introduced to the flow 5 to 50 cm downstream from the dc discharge. Typical operating conditions of the discharge are 3 kV and 30 mA in a mixture of 5 to 15% argon in helium as the main flow gas. Production of $Mn^+(D_2O)_x$ (x = 1–3) was also achieved by a second method, in which He^+ and He^* are formed in a microwave discharge and react further downstream with a volatile metal carbonyl compound to form $Mn(CO)_x^+$ ions. D_2O is added to the flow and $Mn^+(D_2O)_x$ are formed by ligand exchange reactions. Both $Mn_2(CO)_{10}$ and $Mn(CO)_5COCF_3$ were used as parent compounds.[15] D_2O was used instead of H_2O when studying the Mn^+ bound system because $H_3O^+(H_2O)_2$ has the same m/z as Mn^+. In the third method, developed to generate $Ti^+(D_2O)_x$, methane was added to the flow before adding D_2O. In the absence of methane, Ti^+ reacted with D_2O to form $TiO^+(D_2O)_x$ clusters and no beams of $Ti^+(D_2O)_x$ ($x > 1$) were produced in significant quantity. Initial ligation with methane followed by ligand exchange with D_2O is the postulated mechanism for production of $Ti^+(D_2O)_x$. D_2O was used instead of H_2O when studying the Ti^+ bound system in order to eliminate isobaric interferences between $Ti^+(H_2O)_x$ and $TiO^+(H_2O)_{x-1}$ complexes involving different titanium isotopes.

The flow conditions used in this ion source provide approximately 10^5 collisions between an ion and the buffer gas, which should thermalize the cluster ions both rotationally and vibrationally. We assume that clusters produced in this source are in their ground electronic states and that the internal energy of these clusters is well-described by a Maxwell–Boltzmann distribution of rotational and vibrational states corresponding to 298 K. Previous work from this laboratory, including studies of N_4^+,[16] $Fe(CO)_x^+$ (x = 1–5),[17] $Cr(CO)_x^+$ (x = 1–6),[18] SiF_x^+ (x = 1–4),[19] SF_x^+ (x = 1–5),[20] and $H_3O^+(H_2O)_x$ (x = 1–5),[21] have shown that these assumptions are valid.

Thermochemical Analysis. Theory and experiment[22] have shown that cross sections can be modeled in the threshold region with eq 1,

$$\sigma = \sigma_0 \sum g_i (E + E_i + E_{rot} - E_0)^n / E^m \qquad (1)$$

where σ_0 is an energy independent scaling factor, E is the relative translational energy of the reactants, E_{rot} is the rotational energy of the reactants ($3kT/2$ = 0.039 eV in all cases here), E_0 is the threshold for reaction of the ground vibrational and electronic state, n is an adjustable parameter, and m = 1. The summation is over i which denotes the vibrational states of the cluster ions, g_i is the population of those states ($\sum g_i = 1$), and E_i is the excitation energy of each vibrational state. Because the cluster ions studied here have many low frequency vibrational modes, the populations of excited vibrational levels are not negligible even at 298 K.

In the absence of evidence to the contrary, it is assumed that n and σ_0 in eq 1 are the same for all states. This form of eq 1 is expected to be appropriate for translationally driven reactions[23] and has been found to reproduce reaction cross sections well in a number of previous studies of both atom–diatom and polyatomic reactions,[24,25] including CID processes. Cross sections for CID of $Fe(CO)_x^+$ (x = 1–5),[17] $Cr(CO)_x^+$ (x = 1–6),[18] and $H_3O^+(H_2O)_x$ (x = 1–5)[21] have been shown to be modeled well by eq 1 when reasonable values for vibrational frequencies are employed.

The model of eq 1 is convoluted with the kinetic energy distributions of the reactants,[9] and the parameters σ_0, n, and E_0 are optimized with a nonlinear least-squares analysis to give the best fit to the data. An estimate of the error associated with the measurement of E_0 is obtained from the range of threshold values measured for different data sets with variations of the parameter n, variations associated with uncertainties in the vibrational frequencies, variation of the time clusters are estimated to have to dissociate before detection, and the error in the absolute energy scale.

The threshold energies for CID reactions of $M^+(H_2O)_x$ are converted to 0 K BDEs, $D_0(x)$, by assuming that E_0 represents the energy difference between reactants and products at 0 K.[26] This requires that there are no activation barriers in excess of the endothermicity. This is generally true for ion–molecule reactions and has been explicitly tested a a number of times.[25,27] For the simple bond fission reactions studied here, this

(9) Ervin, K. M.; Armentrout, P. B. *J. Chem. Phys.* **1985**, *83*, 166.
(10) Schultz, R. H.; Armentrout, P. B. *Int. J. Mass Spectrom. Ion Processes* **1991**, *107*, 29.
(11) Chantry, P. J. *J. Chem. Phys.* **1971**, *55*, 2746.
(12) Ervin, K. M.; Armentrout, P. B. *J. Chem. Phys.* **1987**, *86*, 2659.
(13) Burley, J. D.; Ervin, K. M.; Armentrout, P. B. *Int. J. Mass Spectrom. Ion Processes* **1987**, *80*, 153. Sunderlin, L. S.; Armentrout, P. B. *Chem. Phys. Lett.* **1990**, *167*, 188.
(14) Manganese powder is contained in a tantalum metal "boat".
(15) $Mn_2(CO)_{10}$ was obtained from Strem Chemical. $Mn(CO)_5COCF_3$ was synthesized by Dr. F. A. Khan with assistance from Professor T. G. Richmond.
(16) Schultz, R. H.; Armentrout, P. B. *J. Chem. Phys.* **1992**, *96*, 1046.
(17) Schultz, R. H.; Crellin, K. C.; Armentrout, P. B. *J. Am. Chem. Soc.* **1991**, *113*, 8590.
(18) Khan, F. A.; Clemmer, D. C.; Schultz, R. H.; Armentrout, P. B. *J. Phys. Chem.* **1993**, *97*, 7978.
(19) Fisher, E. R.; Kickel, B. L.; Armentrout, P. B. *J. Phys. Chem.* **1993**, *97*, 10204.
(20) Fisher, E. R.; Kickel, B. L.; Armentrout, P. B. *J. Chem. Phys.* **1992**, *97*, 4859.
(21) Dalleska, N. F.; Honma, K.; Armentrout, P. B. *J. Am. Chem. Soc.* **1993**, *115*, 12125.
(22) Aristov, N.; Armentrout, P. B. *J. Am. Chem. Soc.* **1986**, *108*, 1806 and references therein.
(23) Chesnavich, W. J.; Bowers, M. T. *J. Phys. Chem.* **1979**, *83*, 900.
(24) See for example: Sunderlin, L. S.; Armentrout, P. B. *Int. J. Mass Spectrom. Ion Processes* **1989**, *94*, 149.
(25) Armentrout, P. B. In *Advances in Gas Phase Ion Chemistry*; Adams, N. G., Babcock, L. M., Eds.; JAI: Greenwich, 1992; Vol. 1, pp 83–119.
(26) See Figure 1 of ref 21.
(27) Boo, B. H.; Armentrout, P. B. *J. Am. Chem. Soc.* **1987**, *109*, 3459. Ervin, K. M.; Armentrout, P. B. *J. Chem. Phys.* **1987**, *86*, 2659. Elkind, J. L.; Armentrout, P. B. *J. Phys. Chem.* **1984**, *88*, 5454. Armentrout, P. B. In *Structure/Reactivity and Thermochemistry of Ions*; Ausloos, P., Lias, S. G., Eds.; Reidel: Dordrecht, 1987; pp 97–164.

Table 1. Vibrational Frequencies and Average Vibrational Energies at 298 K

species	E_{vib},[a] eV	freq (degeneracies), cm^{-1}
$M^+(H_2O)$[b]	0.03(0.01)	302, 363, 438, 1694, 3824, 3913
$M^+(D_2O)$[c]	0.04(0.01)	293, 269, 196, 1178, 2671, 2788
$M^+(H_2O)_2$	0.13(0.02)	12 (2), 59, 216, 338, 337 (2), 419 (2), 1688, 1689, 3829 (2), 3921 (2)
$M^+(D_2O)_2$	0.16(0.02)	12 (2), 31, 210, 329, 150 (2), 310 (2), 1178 (2), 2671 (2), 2788 (2)
$M^+(H_2O)_3$	0.23(0.03)	33 (2), 38, 63 (2), 134, 207, 292 (2), 307, 320 (2), 390, 395 (2), 1682 (2), 1684, 3834 (2), 3835, 3931 (3)
$M^+(D_2O)_3$	0.27(0.03)	32 (2), 37, 33 (2), 70, 201, 283 (2), 137, 143 (2), 289, 293 (2), 1178 (3), 2671 (3), 2788 (3)
$M^+(H_2O)_4$ (SCF)[d]	0.33(0.04)	10 (3), 30, 47, 87 (2), 124, 184, 212, 278 (2), 294, 288 (3), 329, 373, 393 (2), 411, 1728 (3), 1731, 3778 (3), 3780, 3902 (4)
$M^+(H_2O)_4$ (MP2)[e]	0.34(0.04)	12, 14 (2), 32, 47, 87 (2), 124, 179, 204, 267 (2), 283, 276 (2), 278, 309, 358, 376 (2), 394, 1683 (3), 1675, 3800 (4), 3900 (4)
$M^+(D_2O)_4$	0.37(0.04)	12, 14 (2), 31, 45, 46 (2), 65, 94, 198, 259 (2), 275, 123 (2), 124, 138, 265, 279 (2), 292, 1178 (4), 2671 (4), 2788 (4)

[a] Determination of the uncertainties, listed in parentheses, is described in the text. [b] MP2 frequencies calculated using a TZ2P basis set for $M^+(H_2O)_x$ (x = 1–3) are taken from ref 29. [c] The procedure for estimating $Na^+(D_2O)_x$ frequencies is described in the text. Frequencies of vibrational modes for $M^+(D_2O)_x$ are listed in the same order as for $Na^+(H_2O)_x$. [d] SCF frequencies calculated using a TZ2P basis set taken from ref 29. [e] MP2 frequencies calculated using DZ + d basis set corrected as suggested in ref 29.

Table 2. Empirical Analysis of the Ratio of Stretching Frequencies of $Cu^+(H_2O)_x$ Clusters to Those of $Na^+(H_2O)_x$ Clusters

	$Na^+(H_2O)_x$		$Cu^+(H_2O)_x$		
x	μ[a]	D_e[b] (kcal/mol)	μ[c]	D_e[d] (kcal/mol)	$[(\mu/D_e)_{Na}/(\mu/D_e)Cu]^{1/2}$
1	10.10	24.7	14.04	40.5	1.09
2	12.51	22.1	14.76	41.3	1.26
3	13.79	18.4	15.25	16.7	0.91
4	14.59	15.0	15.62	14.5	0.95

[a] Reduced mass of $[Na^+(H_2O)_{x-1} - H_2O]$ in amu. [b] D_es calculated at the SCF level from ref 29. [c] Average reduced mass of $[Cu^+(H_2O)_{x-1} - H_2O]$ for ^{63}Cu and ^{65}Cu in amu. [d] D_es calculated at the MCPF level from ref 8.

assumption should be valid although there is the possibility that dissociation occurs to an excited electronic state asymptote, as discussed further below.

Vibrational Frequencies. The Beyer–Swinehart algorithm[28] is used to calculate the distribution of vibrational energy at 298 K from the vibrational frequencies listed in Table 1. Given the dearth of experimentally determined vibrational frequencies of transition metal ion water clusters, we use vibrational frequencies of $Na^+(H_2O)_x$ calculated by Bauschlicher et al.[29] This substitution is suggested by the electrostatic nature of the bonding in both cases, although the vibrational frequencies of transition metal ion water clusters could differ from those of sodium ion water clusters due to several effects. Transition metal ions have low energy vacant or half-filled d-orbitals that allow electron donation from the water ligands. As ligands are added to the metal ion, orbital hybridization and spin pairing of electrons can occur in the d-orbitals thereby modifying the ion–water bonding. The ionic radius of transition metal ions differs from that of sodium ions, influencing bond length, BDE, and vibrational frequency. The reduced mass of the transition metal ion bound clusters differs from that of the sodium ion bound clusters, further modifying the vibrational frequency. The differences in reduced mass and BDE can be evaluated quantitatively. In Table 2, the reduced masses and BDEs determined theoretically[7,8] are summarized for sodium and copper ion bound water clusters. For a Morse potential, the frequency is proportional to $(\mu/D_e)^{-(1/2)}$, where D_e and μ are the equilibrium bond energy and reduced mass, respectively. Thus, the metal water stretching frequencies of $Na^+(H_2O)_x$ can be related to those of $Cu^+(H_2O)_x$ by $[(\mu/D_e)_{Na}/(\mu/D_e)_{Cu}]^{1/2}$, also shown in Table 2. The ratios of metal–water stretches for each cluster size are within ~25% of unity. On this basis, we have used vibrational frequencies of Na^+–water clusters for all transition metal ion bound water clusters, as summarized in Table 1. No scaling was applied to these ab initio frequencies before use because the level of theory applied in both cases should adequately describe the vibrations of a predominantly electrostatic interaction.[29,30] Although it would be appropriate to scale the internal modes of water, we have not done so here. This choice introduces a negligible error in the final results because the internal modes of water are too high in energy to make a significant contribution to the excited state population of the clusters at 298 K.

We have estimated the sensitivity of our analysis to the deviations from the true frequencies as described in our work on $H_3O^+(H_2O)_x$.[21] All of the vibrational frequencies except for the internal modes of water were scaled by ±25%, and the corresponding change in the *average* vibrational energy is taken to be an estimate of one standard deviation of the uncertainty in vibrational energy and is included in the uncertainties of E_0.

For the purpose of interpreting the CID of $M^+(D_2O)_x$ species, we have estimated the frequencies of $Na^+(D_2O)_x$ from those calculated for $Na^+(H_2O)_x$ on a mode-by-mode basis. Modes stemming from hindered rotations of water molecules are scaled by the ratio of the appropriate rotational constant.[31] Hindered translational modes are scaled by the square root of the ratio of reduced masses of $Na–H_2O$ and $Na–D_2O$.[32] Frequencies corresponding to internal modes of H_2O are replaced with the internal modes of D_2O. Values of E_0 thus obtained from the CID of $M^+(D_2O)_x$ clusters are then corrected for the differences in zero-point energies in order to report BDEs for $M^+(H_2O)_x$. The zero-point energies of $M^+(H_2O)_x$ are larger than those of $M^+(D_2O)_x$ by 0.04 ± 0.01 eV for x = 1–4.

Temperature Assumptions in the Thermochemical Analysis. Equation 1 explicitly includes the internal energy of the cluster ion, E_l and E_{rot}. All energy available is treated statistically, which seems reasonable because both rotational and vibrational energy of the reactants are redistributed throughout the cluster upon impact with the collision gas. The threshold for dissociation is by definition the least amount of energy necessary to effect dissociation and corresponds to formation of products with no internal energy. Hence we refer to eq 1 as the 0 K model. The assumption that products formed *at threshold* have an internal temperature of 0 K has been explicitly tested for metal carbonyl ions[17,18] and $H_3O^+(H_2O)_x$ (x = 1–5),[21] where it was shown that treating all energy of the cluster, translational, rotational, and vibrational, as able to couple into the dissociation coordinate leads to reasonable thermochemistry while other assumptions do not.

In our study of $H_3O^+(H_2O)_x$ (x = 1–5), we considered whether replacing the explicit *distribution* of vibrational energies in eq 1, i.e., the summation over g_iE_i, with the average vibrational energy, E_{vib}, yields acceptable results.[21] Comparison with literature values showed that this average vibrational energy approximation did not yield acceptable results for $H_3O^+(H_2O)_x$ (x = 3–5). Nonetheless, we evaluate this alternate approximation here for $Cu^+(H_2O)_x$, where there is equilibrium and theoretical data for comparison in order to ascertain whether it is a useful approximation in CID studies of transition metal complexes.

Another model for CID cross sections is given in eq 2,

(28) Beyer, T.; Swinehart, D. F. *Comm. Assoc. Comput. Machines* **1973**, *16*, 379. Stein, S. E.; Rabinovitch, B. S. *J. Chem. Phys.* **1973**, *58*, 2438. Stein, S. E.; Rabinovitch, B. S. *Chem. Phys. Lett.* **1977**, *49*, 183. Gilbert, R. G.; Smith, S. C. *Theory of Unimolecular and Recombination Reactions*; Blackwell Scientific Publications: Oxford, 1990.

(29) Bauschlicher, C. W., Jr.; Langhoff, S. R.; Partridge, H.; Rice, J. D.; Komornicki, A. *J. Chem. Phys.* **1991**, *95*, 5142.

(30) Bauschlicher, C. W., Jr., personal communication.

(31) Rotational contants for H_2O were taken from the following: Shimanouchi, T. *Tables of Molecular Vibrational Frequencies*; U.S. Government Printing Office: Washington, DC, 1972; *Consolidated Vol. I*, NSRDS-NBS 39. Rotational constants for D_2O were calculated from the bond length and angle listed therein. The rotational constants ratios, $B(H_2O)/B(D_2O)$, obtained are 1.92, 1.35, and 2.24 for rotation about the C_{2v} symmetry axis, in-plane rotation, and out-of-plane rotation, respectively.

(32) The reduced masses of $Na^+–H_2O$ and $Na^+–D_2O$ were used to obtain the scaling factor 0.972.

$$\sigma = \sigma_0(E - E_{298})^n/E \quad (2)$$

which we term the 298 K model. In contrast to the 0 K model, the 298 K model is based on the assumption that all vibrational and rotational energy is decoupled from the dissociation coordinate, and that only kinetic energy from the collision can drive the dissociation. We compare the results of interpreting cross sections for the loss of one water from $Cu^+(H_2O)_x$ ($x = 1$–4) determined with the 0 K model, eq 1, to those determined with the 298 K model, eq 2.

Dissociation Lifetimes. Another consideration in the analysis of CID thresholds is whether dissociation occurs within the time scale of the experiment, approximately 10^{-4} s in our instrument. If the lifetime of the collisionally excited clusters exceeds this, then the apparent thresholds will be shifted to higher kinetic energies. We have previously detailed how to include consideration of this effect in our threshold analysis by incorporating RRKM theory in eq 1.[18,33] In short, a dissociation probability is determined, and the result of eq 1 is integrated over this probability. The only information required to calculate this dissociation probability is the set of vibrational frequencies appropriate to the transition state for dissociation. This set of frequencies is derived from the vibrational frequencies listed in Table 1 by removing the metal–water stretch frequency that becomes the dissociation coordinate and reducing the frequencies corresponding to the hindered rotations of the water molecule being lost from the cluster. We have arbitrarily reduced the frequencies for the hindered rotations by a factor of 2. This is comparable to the treatment given $Cr(CO)_x^+$ ($x = 5, 6$).[18]

In the present study, we find no appreciable kinetic shifts for $M^+(H_2O)_x$ ($x = 1$–3), while for $x = 4$, the shift is only 0.03 eV. All of the thresholds determined below for $x = 4$ clusters include these corrections and the uncertainties in these values include the effects of increasing and decreasing the time scale (10^{-4} s) by a factor of 2.

Collision Gas. We have used the monatomic gas xenon as the neutral target gas to avoid the issue of transfer of internal energy to or from a molecular gas. Xenon has the further advantage that it is more polarizable than lighter rare gas atoms, providing for a more efficient transfer of kinetic energy into the cluster.[34,35] Its greater mass allows us to work at lower energies in the laboratory frame, ensuring attainment of high collection efficiencies of the product ions. For CID of $Cu^+(H_2O)_4$, argon was also used as a collision gas. In this case, working at higher energies in the laboratory frame moved the threshold region for CID away from the region where the ion beam is truncated, improving the quality of the data without sacrificing the efficiency of product ion collection.

Pressure Effects. Equations 1 and 2 only model cross sections that represent products formed as a result of a single collision. In the present experiments, the pressure of the xenon collision gas, $P(Xe)$, is generally kept sufficiently low that multiple collisions with the ions are rare, but even under such conditions the effects of multiple collisions can be significant, as demonstrated in previous work from our laboratory.[21,36,37] We have verified that such pressure effects become more pronounced for $M^+(H_2O)_x$ ($x = 2$, 3), and similar to our results for $H_3O^+(H_2O)_x$ ($x = 4$ and 5), pressure effects are minimal in the $M^+(H_2O)_4$ clusters when $P(Xe)$ is kept sufficiently low that the product intensity is ≤10% of the reactant beam intensity.

In order to obtain cross sections representative of single collision conditions, we collect data at two or more pressures and then extrapolate the data to zero pressure.[17] Several data sets are collected with a low pressure of xenon, typically $P(Xe) \simeq 0.05$ mTorr, and several data sets are collected with $P(Xe)$ as high as possible without attenuating the reactant ion beam intensity by more than 10%, ~0.15 mTorr for $x = 2$ and 3. Each pair of high- and low-pressure cross sections is linearly extrapolated to zero pressure, rigorously single collision conditions, at each energy. The thresholds reported for $x = 1$–3 in this work are determined from data extrapolated to zero pressure in this manner. Extrapolation was not necessary for most $M^+(H_2O)_4$ data sets. Because the magnitude and even the presence of these pressure effects is difficult to predict, we find it is necessary to perform pressure dependent studies of a cross section in all cases.

(33) Loh, S. K.; Hales, D. A.; Lian, L.; Armentrout, P. B. *J. Chem. Phys.* **1989**, *90*, 5466.
(34) Aristov, N.; Armentrout, P. B. *J. Phys. Chem.* **1986**, *90*, 5135.
(35) Hales, D. A.; Armentrout, P. B. *J. Cluster Sci.* **1990**, *1*, 127.
(36) Lian, L.; Su, C.-X.; Armentrout, P. B. *J. Chem. Phys.* **1992**, *96*, 7542.
(37) Lian, L.; Su, C.-X.; Armentrout, P. B. *J. Chem. Phys.* **1992**, *97*, 4072, 4084.

Results

General. Collision-induced dissociation (CID) spectra were recorded for clusters of one to four water molecules bound by monopositive titanium, vanadium, chromium, manganese, iron, cobalt, nickel, and copper ions. $Ti^+(D_2O)_x$ and $Mn^+(D_2O)_x$ were studied for reasons discussed above. The only processes observed in all systems over the energy range studied (typically 0–5 eV) are the sequential loss of water molecules and ligand exchange with $M^+(H_2O)$ to form M^+Xe ions. Although ligand exchange probably occurs for larger clusters as well, the mass of the product formed when $x \geq 2$ exceeds the available mass range of our quadrupole mass filter and thus we did not collect this product. Other possible products are $MO^+(H_2O)_y$, $MOH^+(H_2O)_y$, and $MH^+(H_2O)_y$ where $y < x$. No evidence for efficient formation of any of these products within the energy range studied was observed. Observation of these products could be obscured by the reactant ion beam or the major products under the resolution conditions used in this study. However, $Ti^+(H_2O)$ and $V^+(H_2O)$ were studied under sufficiently high mass resolution conditions that MO^+, MOH^+, and MH^+ could be observed if formed in quantities on the order of 10% of the cross section of M^+. The failure to observe such species can be rationalized because O–H bond activation processes are kinetically disfavored compared to water dissociation and thermodynamically disfavored for all but the early transition metals[38] and the orientation of the water ligand in the complexes makes formation of such products difficult.

$Cu^+(H_2O)_x$. Because of the availability of equilibrium data for $x = 3$ and 4,[2] other CID values for $x = 1$ and 2,[4,5] and theoretical calculations for $x = 1$–4,[7] we discuss our analysis of the copper ion system in detail as a model system. Cross sections for the CID of $Cu^+(H_2O)_x$ ($x = 1$–4) are shown in Figure 1. The cross section of $Cu^+(H_2O)$, shown in Figure 1a, rises sharply from an apparent threshold of about 1.5 eV. At higher energies, the cross section remains fairly constant, above 3 Å^2 up to the highest energy studied, 5 eV.

In CID of $Cu^+(H_2O)_2$, Figure 1b, the major process is the loss of one H_2O molecule to form $Cu^+(H_2O)$, rising from an apparent threshold near 1.3 eV and reaching about 10 Å^2 by 3 eV. The cross section for formation of Cu^+ in this system rises slowly from an apparent threshold near 3 eV. Formation of Cu^+ is over 200 times less efficient than the loss of one water at 5 eV.

The CID cross section for the loss of one water from $Cu^+(H_2O)_3$, Figure 1c, is nonzero at zero kinetic energy, a result explained by the population of the low-frequency vibrational modes in this cluster ion. Such an observation makes it clear that it is essential to analyze the CID data by taking into account the population of these vibrational states at 298 K, as done in eq 1. The apparent threshold for CID is much lower than those for loss of one water from $Cu^+(H_2O)$ and $Cu^+(H_2O)_2$, indicating that the third water is bound much less strongly to the Cu^+ ion than the first and second water. The cross section is also very large, reaching 36 Å^2 at 1.5 eV, declining thereafter to about 28 Å^2 at 5 eV. This decline is largely compensated by the cross section for the loss of two water ligands, which rises from an apparent threshold near 2.2 eV. This process is only about five times less efficient than the primary dissociation channel. The loss of all three water ligands was not observed in the energy range studied.

The CID spectrum of $Cu^+(H_2O)_4$ is shown in Figure 1d, and again exhibits a nonzero cross section at zero kinetic energy. The cross section of this process reaches a maximum of 33 Å^2 by 1 eV, where it begins to decline due to loss of another water molecule. By 5 eV, this cross section has fallen to 20 Å^2. The cross section for the loss of two water molecules rises from an apparent threshold at about 0.8 eV, reaching 14 Å^2 by 3.5 eV and remaining constant

(38) Although the thermochemistry of *hydrated* MO^+, MOH^+, and MH^+ species is as yet uncharacterized, it seems unlikely that the thermodynamics of these species relative to $M^+(H_2O)_x$ species will change appreciably from the unligated case where the thermodynamics is known.

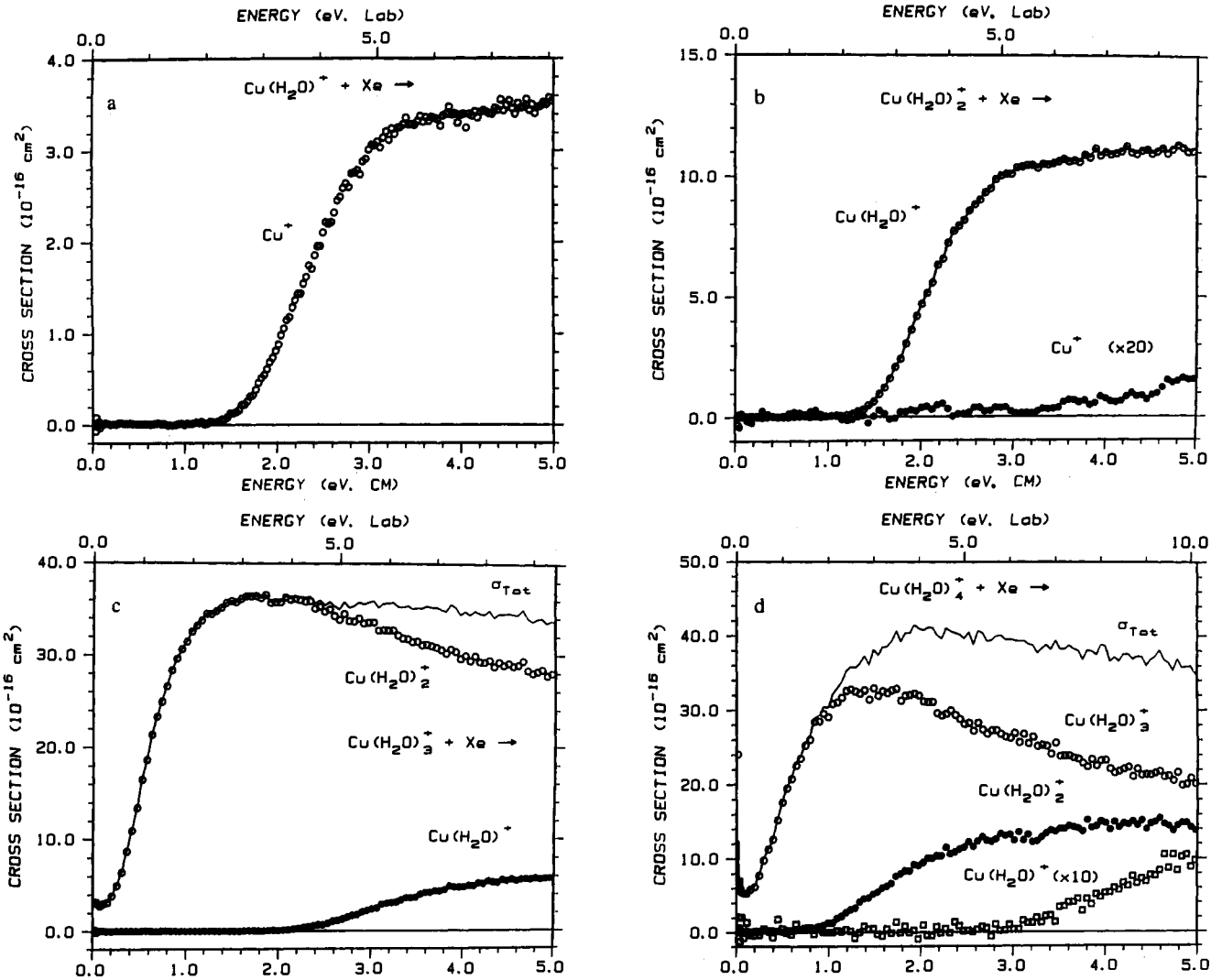

Figure 1. Parts a–d show cross sections for CID of $Cu^+(H_2O)_x$ (x = 1–4), respectively, as a function of relative kinetic energy (lower x axis) and laboratory energy (upper x axis). The solid line shows the total cross section for dissociation.

to 5 eV. The apparent threshold for the loss of three water molecules is near 3.0 eV. This cross section rises to only 1.0 Å^2 at 5 eV. Loss of four ligands is not observed in this energy range.

The CID cross section and the best 0 K model function, eq 1, are shown in the threshold region in Figure 2 for $Cu^+(H_2O)_2$. Note that the 0 K model reproduces the experimental cross section for over two orders of magnitude and for a energy range of about 1.6 eV. The quality of this reproduction of the data is typical for all cross sections measured here. The best fit parameters of eq 1 for x = 1–4 are summarized in Table 3.

Primary thresholds of $Cu^+(H_2O)_x$ (x = 1–4) were also analyzed with the average vibrational energy approximation and 298 K models and the results are listed in Table 4. Results obtained from modeling the CID cross section of $Cu^+(H_2O)$ by using the 0 K model, eq 1, and the 0 K average vibrational energy approximation agree well with both theory and the results of MDM. The 298 K model, eq 2, yields a result that is lower and outside the combined uncertainties. The measured thresholds for loss of H_2O from $Cu^+(H_2O)_2$ are similar for the 0 K model and the average vibrational energy model. Again, the 298 K model is outside the combined uncertainty of the 0 K average energy approximation. The theoretical result of RB falls between the 298 K model result and the 0 K model results, but MDM report a value more in line with the 0 K model. The threshold for CID of $Cu^+(H_2O)_3$ measured using the 0 K model is in good agreement with both the prediction of theory and the result of HC and MDM. The result from the average vibrational energy approximation of the 0 K model no longer agrees with the 0 K model result, and the 298 K model yields a value lower still. The same trend is reflected in the results for x = 4. Results from the average vibrational energy approximation and the 298 K models differ from the 0 K result by less for x = 4 than for x = 3 because here the other models do not account for lifetime effects while the 0 K model does. Accounting for lifetime effects in the other models would lower those results further. The 0 K result for x = 4 is in good agreement with both the prediction of theory and the result of MDM. The best qualitative agreement between the present work and the result of HC is given by the 0 K model, the highest result of the three models tested. Based on agreement with the results of HC and the theoretical predictions of RB, we conclude that the best interpretation of CID data is obtained with the 0 K model. The limitations of the 298 K and average vibrational energy models are clearly shown by the results for x = 3 and 4.

Secondary Thresholds. Sequential BDEs can also be determined from the difference between thresholds of two successive ligand loss processes. For example, the difference between the thresholds for reactions 3 and 4 is, in principle, equal to $D_0(x)$.

$$M(H_2O)_x^+ \rightarrow M(H_2O)_{x-1}^+ + H_2O \quad (3)$$

$$M(H_2O)_x^+ \rightarrow M(H_2O)_{x-2}^+ + 2H_2O \quad (4)$$

BDEs determined in this fashion from the present data for $Cu^+(H_2O)_x$ (x = 3 and 4) are given in Table 5. Because one of the potential advantages of obtaining thermochemistry from sec-

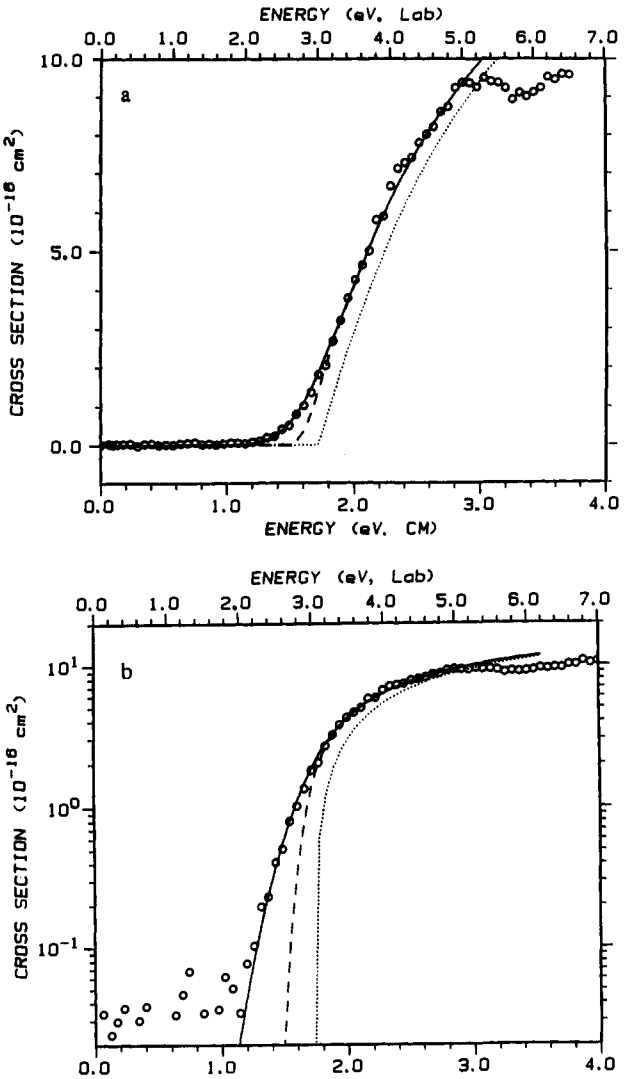

Figure 2. Threshold for CID of $Cu^+(H_2O)_2$ as a function of relative kinetic energy. Open circles show the cross section extrapolated to zero collision gas pressure shown on linear (part a) and semilog (part b) plots. The best fit of eq 1 (dashed lines) is shown convoluted over the neutral and ionic kinetic energy distribution (solid line). The unconvoluted model for 0 K reactants is also shown (dotted line).

ondary thresholds is that the internal energy of the cluster can be neglected, we interpret these thresholds by using eq 2. Data extrapolated to zero pressure were analyzed so that the choice of an arbitrary pressure, which would skew the results, would be avoided. Table 5 clearly shows that the BDEs determined from primary vs secondary ligand loss processes do not lie within the uncertainties of BDEs determined from primary thresholds.

These differences may be explained by several systematic errors in the measurement of secondary and tertiary thresholds. First, the lifetime for loss of two or more waters must be longer than for loss of one water, and therefore can increase the kinetic shift. Second, pressure effects, which lower observed thresholds due to multiple collisions, are more severe for secondary and tertiary thresholds than for primary thresholds, as amply demonstrated in our studies of metal cluster CID.[36,37] Third, when more than one water molecule leaves the cluster, the formation of dimers or trimers would reduce the total energy required for the process to occur.[39] Although we do not believe this process is likely in these systems, it cannot be ruled out entirely. Thresholds affected by dimer loss would be lowered by the dimerization energy of water at 0 K, calculated to be about 3 kcal/mol.[40,41] Because kinetic shift and multiple-collision effects act on the thresholds in opposite directions, a cancellation of errors may be achieved under propitious experimental conditions. An often cited argu-

(39) A possibility noted for $H_3O^+(H_2O)_x$ clusters by: Magnera, T. F.; David, D. E.; Michl, J. *Chem. Phys. Lett.* **1991**, *182*, 363.

Table 3. Parameters of Eq 1 Used To Analyze CID Cross Sections[a]

x	M	E_0 (eV)	n	σ_0
1	Ti	1.60(0.06)	1.0(0.1)	6.6(0.4)
	V	1.52(0.05)	1.2(0.2)	8.8(0.5)
	Cr	1.34(0.09)	1.3(0.1)	9.5(1.1)
	Mn	1.23(0.06)	1.0(0.1)	7.9(0.3)
	Fe	1.33(0.05)	1.4(0.1)	5.9(1.0)
	Co	1.67(0.06)	1.1(0.1)	6.6(1.1)
	Ni	1.87(0.03)	1.2(0.1)	5.5(0.1)
	Cu	1.63(0.08)	1.5(0.1)	5.4(0.2)
2	Ti	1.41(0.05)	1.0(0.1)	19(2)
	V	1.56(0.10)	1.2(0.3)	25(2)
	Cr	1.47(0.06)	1.2(0.3)	25(5)
	Mn	0.93(0.05)	1.7(0.1)	17(1)
	Fe	1.70(0.04)	1.7(0.1)	16(1)
	Co	1.68(0.07)	1.5(0.1)	23(2)
	Ni	1.74(0.08)	1.3(0.3)	21(1)
	Cu	1.76(0.07)	1.2(0.2)	28(5)
3	Ti	0.69(0.07)	1.3(0.3)	34(3)
	V	0.70(0.05)	1.3(0.1)	53(1)
	Cr	0.52(0.05)	1.0(0.1)	49(7)
	Mn	1.12(0.06)	1.4(0.2)	27(3)
	Fe	0.79(0.04)	1.8(0.1)	28(2)
	Co	0.67(0.05)	0.9(0.2)	37(6)
	Ni	0.70(0.06)	1.1(0.1)	39(1)
	Cu	0.59(0.08)	1.2(0.3)	48(1)
4	Ti	0.87(0.08)	1.0(0.2)	20(3)
	V	0.70(0.08)	1.6(0.2)	58(9)
	Cr	0.53(0.07)	0.6(0.1)	67(11)
	Mn	0.52(0.05)	0.9(0.1)	49(3)
	Fe	0.52(0.07)	0.9(0.1)	66(2)
	Co	0.60(0.06)	0.8(0.1)	60(2)
	Ni	0.54(0.06)	1.0(0.2)	[b]
	Cu	0.48(0.09)	1.2(0.3)	47(7)
	Cu[c]	0.59(0.05)	0.9(0.1)	45(3)

[a] Uncertainties listed in parentheses. [b] Value not reported for reasons described in text. [c] Argon was used as the collision gas.

Table 4. 298 K Bond Enthalpies (kcal/mol) Obtained by Analyzing Data for Reaction 3 (x = 1–4, M = Cu) Using the 298 K, Average Vibrational Energy Approximation, and 0 K Models[a]

x	298 K	average	0 K	RB[b]	MDM[c]	HC[d]
1	33.0(2.0)	35.4(2.0)	38.4(0.2)	38.1	35.0(3.0)	
2	35.3(2.0)	39.3(2.0)	40.7(0.5)	37.9	39.0(3.0)	
3	3.9(1.4)	9.8(1.5)	13.7(1.8)	15.5	17.0(3.0)	16.7(1)
4	5.1(1.2)	11.5(1.5)	12.8(1.0)[e]	13.1	15.0(3.0)	16.4(1)

[a] Uncertainties are listed in parentheses. [b] Ab initio results of Rosi and Bauschlicher, ref 7, adjusted to 298 K values. [c] CID results of Magnera, David, and Michl, refs 4 and 5. [d] Equilibrium results of Holland and Castleman, ref 2. [e] Weighted average of Ar and Xe results from Table 3.

Table 5. $\Delta H(x)$ for Cu^+ Determined from Thresholds of Reactions 3 and 4[a]

reaction	n	E_{298}	x	$\Delta H(x)$[b]
$Cu^+(H_2O)_3 \rightarrow Cu^+(H_2O)_2$	1.3(0.3)	3.9(1.2)		
$\rightarrow Cu^+(H_2O)$	1.2(0.2)	55.1(1.8)	2	51.2(2.5)
				40.7(1.6)
$Cu^+(H_2O)_4 \rightarrow Cu^+(H_2O)_3$	1.2(0.1)	5.1(0.5)		
$\rightarrow Cu^+(H_2O)_2$	1.1(0.2)	23.5(1.6)	3	18.4(1.7)
				13.7(1.8)
$\rightarrow Cu^+(H_2O)$	1.1(0.3)	76.6(2.3)	2	53.0(2.8)
				40.7(1.6)

[a] Uncertainties are listed in parentheses. [b] BDEs determined from primary ligand loss using eq 1 are shown in boldface type for comparison.

(40) Frisch, M. J.; Del Bene, J. E.; Binkley, J. S.; Schaefer, H. F. *J. Chem. Phys.* **1986**, *84*, 2279.

(41) Del Bene, J. E.; Mettee, H. D.; Frisch, M. J.; Luke, B. T.; Pople, J. A. *J. Phys. Chem.* **1983**, *87*, 3279.

ment in favor of determining ligand BDEs from successive thresholds is that the internal energy distribution of the reactant ions can be neglected because the internal energy of the cluster reduces both thresholds by the same amount. However, this is true (at least for thermalized clusters) only if the lifetime and pressure effects (both of which are different for primary vs higher order dissociations) are accurately accounted for.

$M^+(H_2O)_x$, M = Ti to Ni. Primary CID thresholds of other metal ion bound water clusters were analyzed by using the 0 K threshold model in the same fashion as for the copper system. Lifetime effects were considered in the analysis of $x = 4$ as described above. Table 3 lists the best fit parameters of eq 1 to the data. $Ni^+(H_2O)_4$ showed evidence of possible contamination with an excited state of the cluster. This has been observed in $Ni^+(CO)_x$ ($x = 1$ and 2).[42] Corrections for this were made as described in the analysis of $Ni^+(CO)_x$ and consequently a value for σ_0 is not reported.

Discussion

The thresholds listed in Table 3 are taken to equal the 0 K BDEs for all metal ion bound water clusters. These BDEs are then converted to 298 K bond enthalpies by eq 5, where $E_{vib}(x)$

$$\Delta H(x) = D_0(x) - E_{vib}(x) + E_{vib}(x-1) + E_{vib}(H_2O) + 4k_BT \quad (5)$$

is the average vibrational energy of $M^+(H_2O)_x$ at 298 K as listed in Table 1. The $4k_BT$ term accounts for three translational and three rotational degrees of freedom created during the bond breaking process and the $\Delta PV = k_BT$ work term that converts energy to enthalpy. The 298 K bond enthalpies derived are listed in Table 6 and shown graphically in Figure 3. Previous CID,[4-6] equilibrium,[2] and ab initio values[7,8] (the latter are also adjusted to 298 K) are listed with the present results in Table 6. BDEs for the third water ligand are reported for the first time except for vanadium and copper ion bound clusters. BDEs for the fourth water ligand are reported for the first time except in the case of copper ion bound clusters. For clusters with one and two water ligands, the theoretical predictions[7] agree quite well with our results. The average deviation of the present results from theory is less than 0.1 kcal/mol for clusters $x = 1$ and 0.6 kcal/mol for clusters of $x = 2$. The absolute average deviations are 0.9 and 1.5 kcal/mol for clusters of $x = 1$ and 2, respectively.

We will also find it convenient to compare the differences between sequential bond energies in analyzing our experimental results. These differences are given as $\Delta(x,x-1) = \Delta H(x) - \Delta H(x-1)$.

Copper. The various results for copper are discussed above. Here, we note that our value for $\Delta(2,1)$ is within experimental error of theory and is close to that observed by MDM. Also, the sign and magnitude of $\Delta(4,3)$ determined here are comparable to those of BLP,[8] MDM, and HC.

Nickel. Our result for $\Delta H(2)$ agrees well with values from RB, MS, and MDM. For $\Delta H(1)$, however, there is considerable disagreement, as evidenced by the $\Delta(2,1)$ values. We report $\Delta(2,1) < 0$, in accord with theory[7] but in contrast to both MDM[5] and MS,[6] although both MDM and MS are within experimental uncertainty of a negative value.

Cobalt. In this system, all three experimental values and theory agree nicely for $x = 1$. For $x = 2$, the value obtained by MDM is clearly much larger than the other three values as reflected in $\Delta(2,1)$.

Iron. Schultz and Armentrout[43] have reported the sequential BDEs of $Fe^+(H_2O)_x$ ($x = 1$–4). We have reanalyzed the results for $x = 4$ to include the analysis of lifetime effects, consistent with the interpretation used here for other metals. This reanalysis yields a lower BDE, Table 6, because of differences in the vibrational frequencies used to determine the internal energy of the cluster and a more rigorous implementation of RKKM theory used to estimate lifetimes of the energized cluster ions.

This system shows the largest value of $\Delta(2,1)$ of the first-row transition metals. The three experimental numbers are in good agreement for both $x = 1$ and 2, with our numbers falling between

(42) Khan, F. K.; Steele, D. L.; Armentrout, P. B. Manuscript in preparation.
(43) Schultz, R. H.; Armentrout, P. B. *J. Phys. Chem.* **1993**, *97*, 596.

Table 6. Enthalpy Changes at 298 K for Dissociation of First-Row Transition Metal Cation Water Clusters[a]

		$\Delta H(x)$ (kcal/mol) for $x =$				
M	source	1	2	Δ(2,1)	3	4
Ti	DHSA[b]	37.7(1.4)	32.6(1.2)	−5.1	16.0(1.6)	19.9(1.8)
	RB[c]	38.3	33.9	−4.4		
	MDM[d]	38.0(3.0)				
V	DHSA	35.8(1.2)	36.0(2.3)	0.2	16.2(1.1)	16.0(1.8)
	RB	35.5	38.0	2.5		
	MDM	36.2(3.0)				
	MS[e]	35.1(4.0)	35.5(4.0)	0.4	12.2(4.0)	
Cr	DHSA	31.7(2.1)	34.0(1.8)	2.3	12.1(1.2)	12.1(1.4)
	RB	30.9	32.6	1.7		
	MDM	29.0(3.0)				
	MS	21.9(4.0)	29.5(4.0)	7.6		
Mn	DHSA	29.1(1.4)	21.5(1.2)	−7.6	25.9(1.4)	11.8(1.2)
	RB	29.3	21.6	−7.7		
	MDM	26.5(3.0)	17.8(3.0)	−8.7		
	MS	28.5(4.0)	17.1(4.0)	−11.4		
Fe	SA[f]	31.5(1.2)	39.3(1.0)	7.8	18.3(0.9)	11.8(1.6)
	RB	34.5	37.1	2.6		
	MDM	28.8(3.0)	38.0(3.0)	9.2		
	MS	32.8(4.0)	40.8(4.0)	8.0		
Co	DHSA	39.3(1.4)	38.8(1.6)	−0.5	15.5(1.1)	13.7(1.4)
	RB	39.0	39.4	0.4		
	MDM	37.1(3.0)	45.0(3.0)	7.9		
	MS	40.1(4.0)	41.9(4.0)	1.8		
Ni	DHSA	43.9(0.8)	40.2(1.8)	−3.7	16.2(1.5)	12.3(1.5)
	RB	41.9	38.3	−3.6		
	MDM	36.5(3.0)	38.0(3.0)	1.5		
	MS	39.7(4.0)	40.6(4.0)	0.9		
Cu	DHSA	38.4(1.8)	40.7(1.6)	2.3	13.7(1.8)	12.8(1.0)
	RB	38.1	37.8	−0.3	15.4	13.3
	MDM	35.0(3.0)	39.0(3.0)	4.0	17.0(3.0)	15.0(3.0)
	HC[g]				16.7	16.4
Na	DK[h]	23.4	19.2	−4.2	15.2	13.2

[a] Uncertainties are listed in parentheses. [b] This work. Thresholds from Table 3 are adjusted to 298 K. [c] Ab initio results of Rosi and Bauschlicher, ref 7, adjusted to 298 K. [d] CID results of Magnera, David, and Michl, refs 4 and 5. [e] CID results of Marinelli and Squires, ref 6. These results were assumed to correspond to 298 K bond energies. [f] CID results of Schultz and Armentrout, ref 17, adjusted to 298 K. Value for $x = 4$ reinterpreted as described in the text. [g] Equilibrium results of Holland and Castleman, ref 2. No estimate of experimental error is given. [h] Equilibrium mass spectrometry results of Dzidic and Kebarle, ref 1.

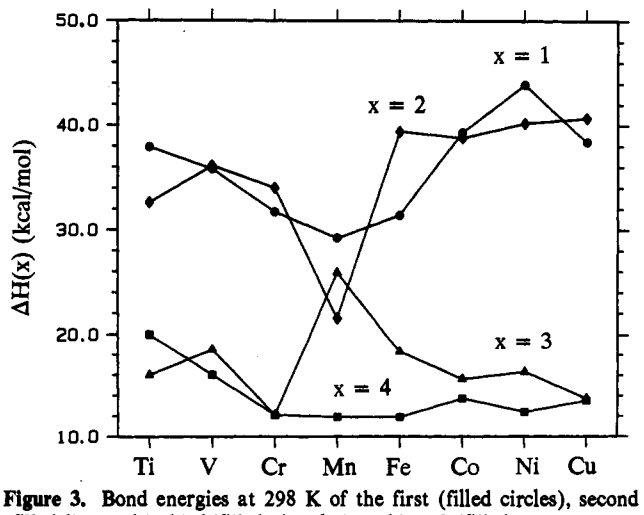

Figure 3. Bond energies at 298 K of the first (filled circles), second (filled diamonds), third (filled triangles), and fourth (filled squares) water ligands bound to transition metal ions determined in this study.

those of MDM and MS. Further, the experimental values for $\Delta(2,1)$ are all in good agreement. In contrast, theory obtains a much lower value of $\Delta(2,1)$, the only case where the theoretical number is outside our experimental uncertainty. One possible explanation for this discrepancy notes that experiment and theory agree on the *sum* of the two bond energies in $Fe^+(H_2O)_2$ (a result also obtained for the other metals; average deviation = –0.5 kcal/mol, absolute average deviation = 1.8 kcal/mol). Given that the calculation for $Fe^+(H_2O)$ is particularly difficult because of nearly degenerate sextet and quartet states, it seems possible that theory has overestimated the first bond energy while underestimating the second (which RB suggest could be up to 2.4 kcal/mol low relative to the first). Alternatively, the spin states of $Fe^+(H_2O)$ may introduce experimental ambiguities, as discussed further below.

Manganese. All three experimental values and theory are in good agreement for $x = 1$, while for $x = 2$, MDM and MS obtain values somewhat lower than our result and theory. This discrepancy is probably related to the fact that the $Mn^+(H_2O)$–H_2O bond is quite weak, the weakest of all $x = 1$ and 2 BDEs. Manganese has the most negative value of $\Delta(2,1)$ of the systems studied here. In contrast, $\Delta H(3)$ for Mn^+ is the strongest BDE for $x = 3$ clusters. The increase in BDEs from $x = 2$ to 3 distinguishes the trend in BDEs of water to Mn^+ from the other first-row transition metal ions.

Chromium. The largest difference between the results of MDM and MS, 7.1 kcal/mol, is seen for $Cr^+(H_2O)$. Our result is in line with that of MDM and theory. Our result for $Cr^+(H_2O)_2$ differs from that of MS by 4.5 kcal/mol and is within experimental error of the theoretical number.

Vanadium. Our results for $x = 1$ and 2 agree well with previous results, as does our value of $\Delta(2,1)$. MS measure $\Delta H(3)$ that is 4.0 kcal/mol *lower* than our value, a result that can be attributed to their use of a 298 K model. Indeed, this difference roughly corresponds to the internal energy of $V^+(H_2O)_3$.

Titanium. Our BDE for $x = 1$ agrees well with theory and MDM, while theory and our value agree nicely for $x = 2$ as well. The increase in BDE from $x = 3$ to 4 sets the trend in BDEs of water to Ti^+ apart from the other first-row transition metals, where $\Delta(4,3)$ values are less than or equal to zero.

Comparison to Previous CID Results. There are a number of differences between the methods of data analysis used in the present study and those used in the previous CID studies of MDM and MS. We believe that these differences could cause systematic errors in the previous studies. This comparison is intended to act as a guide to future research involving CID studies of thermochemistry, rather than as a criticism of these early ground-breaking studies. Michl and co-workers[4,5] did not account for the motion of the neutral reactant[44] and interpreted their data with the parameter n and m of eq 1 held constant at 1.5, a value found to best fit their data when previous threshold results were known. This approach is at odds with our findings that a variety of functional forms (when $m = 1$, n varies from ~0.5 to 1.9, Table 3) are needed in order to adequately reproduce our data (although Magnera and Michl suggest that this difference may be appropriate because their clusters are not thermalized, with levels close to the dissociation limit heavily populated[45]). Because their clusters had elevated internal energies, of necessity, MDM used differences between primary and secondary thresholds to determine BDEs (and made no mention of accounting for pressure effects, although they did operate at a pressure leading to <5% of first fragment loss[45]). As demonstrated here for thermalized clusters, secondary thresholds are susceptible to systematic errors, such as those due to kinetic shifts and multiple collisions. MS interpreted primary thresholds by using a linear cross section model ($n = 1$, $m = 0$) with a Doppler correction[11] and assumed the threshold corresponded to a temperature of 298 K. Internal energy of the cluster and the effects of multiple collisions were not accounted for. Their model is related to our 298 K model assumption, although it differs in that the functional form is arbitrarily chosen and the threshold region of their cross sections is not reproduced because of instrumental limitations.[46] Because the overall agreement of these studies with our results is reasonable in most cases, it appears that the various assumptions made in the previous two studies were not unreasonable, largely because these assumptions lead to fairly small changes in the thresholds for the small metal–ligand complexes, $M^+(H_2O)$ and $M^+(H_2O)_2$. We think it likely that some fortuitous cancellation of errors occurs when thermochemistry is determined from secondary thresholds and when pressure effects, kinetic shifts, and the internal energy of the clusters are not explicitly considered.

Trends in Sequential BDEs. The trends in sequential BDEs of water to the transition metal ions can be contrasted with that for sodium, Table 6, where the BDEs decrease gradually as the number of ligands increases. Most of the transition metal ion bound water clusters have similar patterns in the sequential BDEs: fairly similar values for $x = 1$ and 2, a sharp decrease to $x = 3$, and a slight decrease to $x = 4$. For titanium, manganese, and nickel, the BDEs decrease from $x = 1$ to 2; while for iron, the $x = 1$ BDE is lower than the $x = 2$ BDE. Manganese is clearly distinct because the BDEs increase from $x = 2$ to 3 and then decrease strongly to $x = 4$. Titanium is odd because it exhibits a significant increase from $x = 3$ to 4.

Periodic Trends and Bonding Mechanisms across the Transition Row. Trends across the transition row are illustrated graphically for each value of x in Figure 3. Bonding in $M^+(H_2O)_x$ ($x = 1$ and 2) has been described by RB based on their ab initio calculations. The BDEs between a metal cation and water ligands are governed by a balance between ion–dipole attraction and Pauli repulsion between the ligand and the ion.[7] The Pauli repulsion can be reduced by a number of mechanisms, including 4s–3dσ hybridization, 4*s*–4*p* polarization, or possibly reduction in spin of the metal ion. RB note that the d orbitals in pseudolinear symmetry (linear MO for $x = 1$ where the symmetry axis is z and the molecule lies in the xz plane) on the metal ion are ordered $3d\delta(xy) \approx 3d\delta(x^2 - y^2) < 3d\pi(yz) < 3d\pi(xz) < 3d\sigma$. The 4s orbital of the metal overlaps with the σ lone pair of water, but this metal–ligand repulsion can be reduced somewhat by polarization. On the left side of the transition row 3d–4s promotion with 4s–4p polarization serves to increase the $x = 1$ BDE. Moving from left to right across the periodic table, electrons are "added" to the next least repulsive orbital of the metal. The decrease of $x = 1$ BDEs from titanium to manganese reflects this increasing occupation. Adding more electrons forces double occupation of orbitals. In manganese and iron, this combines with 4s–4p polarization to increase the BDE. The 4s orbital is no longer occupied in the ground states of cobalt and nickel ions, identifying the cause for the further increase in BDE. In $Cu^+(H_2O)$, there are no 3d holes and thus the BDE is reduced from $Ni^+(H_2O)$.

The BDEs of the $x = 2$ clusters are fairly constant (excluding Mn), with those for early transition metals being somewhat smaller than those for later transition metals. We attribute this change as due to the contraction of the 3d orbitals on the right side of the transition row. This is reflected in the metal–water bond distances calculated by RB, ~4.0 Å for Ti to Cr and ~3.7 Å for Fe to Cu. RB point out that 4s–3dσ hybridization continues to

(44) Reference 4 ignores the Doppler broadening because they calculate it to be only 0.2 eV at 300 K and 2 eV center-of-mass energy, much smaller than the 1 eV fwhm distribution of the ions. In contrast, we calculate that under these conditions, for reaction of $Cu^+(H_2O)_2$ with butane (the most favorable case), the fwhm of the Doppler broadening according to the equations given by Chantry[11] is 0.6 eV, more comparable to the ion energy distribution. It would appear that the correct fwhm in the center-of-mass frame of 0.6 eV was thought to be in the laboratory frame, and then inappropriately "corrected" to the center-of-mass frame yielding the stated fwhm of 0.2 eV.

(45) Magnera, T.; Michl, J. Personal communication.

(46) Squires, R. R. Personal communication.

play a leading role in the BDEs of $x = 2$ clusters. The $x = 2$ BDE for manganese is obviously anomalous. Because of the large promotion energy required to achieve 4s–3dσ hybridization (the $^5S(4s^13d^5)$ and $^5D(3d^6)$ states of Mn^+ lie 27 and 41 kcal/mol,[47] respectively, above the $^7S(4s^13d^5)$ ground state), a bent OMO structure is adopted and 4s–4p polarization reduces the repulsion between the occupied 4s orbital and the ligands.

Except for the manganese system, the metal–water BDEs for all metals studied here drop significantly from $x = 2$ to 3. BLP suggest that this large drop in the $Cu^+(H_2O)_x$ system arises from the increase in ligand–ligand repulsion and the loss of 4s–3dσ hybridization. A similar rationale seems likely to hold for many of the other metals, although these metals may retain some 4s–3dσ hybridization because only one electron need occupy the hybrid orbitals. This may rationalize why the $x = 3$ BDEs for most metals exceed that of Cu.

While most $x = 3$ BDEs lie between 12 and 18 kcal/mol, the $x = 3$ BDE for M = Mn is much higher. We rationalize this observation by suggesting that $Mn^+(H_2O)_3$ has a quintet spin ground state which allows 4s–3dσ hybridization. This removes electron density from the 4s orbital occupied in $Mn^+(H_2O)_x$ ($x = 1$ and 2), thereby reducing the metal–ligand repulsion and increasing the BDE. The promotion energy necessary to access the quintet state (noted above) is paid largely by the first two water ligands, as shown by the theoretical prediction that the septet–quintet splitting energy in the $Mn^+(H_2O)_2$ cluster is small (4.4 kcal/mol).[7]

Most $x = 4$ BDEs decrease slightly from the $x = 3$ BDEs, presumably due to increased ligand–ligand repulsion. Manganese shows a large drop, but this can be attributed to its anomalously high $x = 3$ BDE. The $x = 4$ BDE for Ti is the largest value and shows an increase from $x = 3$ to 4. This may be because of a change in spin to a doublet state.

Geometries of $x = 3$ and 4 Clusters. Calculations predict that both $Na^+(H_2O)_3$ and $Cu^+(H_2O)_3$ have D_{3h} symmetry.[8,29] In this planar arrangement of ligands, the relative ordering of the d-like molecular orbitals (mos) is $3d(xz) = 3d(yz)$ (–2.57 *Dq*) < $3d(z^2)$ (–0.65 *Dq*) < $3d(xy) = 3d(x^2 - y^2)$ (2.895 *Dq*), where the *z* axis is the symmetry axis, and the relative energies of the orbitals are from Krishnamurthy and Schaap.[48] The 4s-like mo is quite high in energy and is not expected to be populated in the $M^+(H_2O)_3$ clusters. As electrons are removed from the spherically symmetric $Cu^+(3d^{10})$ configuration, the molecules will distort from D_{3h} due to Jahn–Teller effects. Such distortions will be opposed by ligand–ligand repulsion. The propensity for strong distortions can be estimated from the relative energies of the populated d orbitals, although this assumes that the M–O bond lengths do not change appreciably. If the splitting in mos is sufficiently large, it is possible that it will be energetically favorable to change from a high-spin $3d^n$ configuration to a lower-spin state, but prediction of this requires absolute measure of the mo splitting energy, which is unavailable.

As electrons are removed from the $(3d\pi)^4(3d\sigma)^2(3d\delta)^4$ configuration of $Cu^+(H_2O)_3$, nickel ($3d^9$) and cobalt ($3d^8$) should distort from D_{3h} symmetry but the stabilization is relatively small, such that doublet and triplet states, respectively, of near D_{3h} symmetry are anticipated. For Fe^+ ($3d^7$), the stabilization upon distortion is more substantial (1.14 *Dq* units for the quartet state), and the possibility that the doublet state (where the highest 3d mo is unoccupied) may be the ground state should be considered. Likewise, the quintet Mn^+ ($3d^6$) state should distort strongly, and a triplet state could leave the highest 3d mo unoccupied. Sextet Cr^+ ($3d^5$) should not distort, although some stabilization might be acquired by reducing to a quartet spin state. Quintet V^+ ($3d^4$) and quartet Ti^+ ($3d^3$) show little stabilization upon distortion from planar geometry; however, the stabilization attained by doublet titanium upon distortion is appreciable (1.7 *Dq* units).

RB predict a tetrahedral MO_4 arrangement in both $Na^+(H_2O)_4$ and $Cu^+(H_2O)_4$. We compare tetrahedral to square-planar geometries by again making use of the information provided by Krishnamurthy and Schaap.[48] For a tetrahedral complex, the $3dz^2$ and $3d(x^2 - y^2)$ orbitals are degenerate (–2.67 *Dq*) and lower than the $3d(xy)$, $3d(xz)$, $3d(yz)$ orbitals which are also degenerate (1.78 *Dq*). The square-planar ligand field (with ligands along the *x* and *y* axes) has $3d(xz) = 3d(yz)$ (–3.43 *Dq*) < $3d(xy)$ (–1.14 *Dq*) < $3d(z^2)$ (–0.86 *Dq*) < $3d(x^2 - y^2)$ (8.86 *Dq*). Doublet Ni^+, triplet and singlet Co^+, and both quartet and doublet Fe^+ show strong stabilization as undistorted square planes. Quintet manganese should distort from either tetrahedral or square-planar geometry, and shows a slight preference for square-planar geometry. Triplet manganese should distort from either tetrahedral or square-planar geometry and shows a 5.17 *Dq* preference for the latter. The sextet state of Cr^+ is expected to have an undistorted tetrahedral geometry, while a quartet state should distort from square-planar geometry. Quintet vanadium and both quartet and doublet titanium are more stable in square-planar than tetrahedral geometry by 7.1, 2.3, and 2.3 *Dq* units, respectively.

Spin Effects. Although CID provides no direct information about the spin or electronic state of the metal ion, trends in sequential BDEs have been used to infer spin changes at the metal ion center as the number of CO ligands solvating gaseous iron[17] and chromium[18] ions is varied. A potential difficulty arises when the cluster under study has a spin state different from that for the ground state of the dissociation products. If the cluster dissociates adiabatically, then CID measures the true BDE. If the cluster dissociates diabatically, along a spin-allowed pathway to form excited product ions, then the threshold measured is higher than the adiabatic BDE by the energy difference between the ground and excited state asymptotes. This particular dilemma has been discussed in detail for CID of $FeCO^+$.[17]

Theory[7,8] predicts the ground states of all $x = 1$ clusters studied here to have the same spin as the ground state of the isolated metal ion. Therefore, all these BDEs should correspond to the adiabatic bond energies. Spin changes are theoretically predicted for $Fe^+(H_2O)_2$ but no other $x = 2$ clusters. Theory predicts $Fe^+(H_2O)_2$ to be quartet spin. If $Fe^+(H_2O)_2$ dissociated to form quartet $Fe^+(H_2O)$ then the BDE measured for $Fe^+(H_2O)_2$ would be too high by the sextet–quartet splitting in $Fe^+(H_2O)$. Calculations indicate that this splitting is less than 4.4 kcal/mol and may be as little as 0.8 kcal/mol.[7] Decreasing $\Delta H(2)$ for Fe^+ by 0.8 to 4.4 kcal/mol would improve the agreement between our experimental value of $\Delta(2,1)$ and that of theory, Table 6. A similar situation exists for $Mn^+(H_2O)_3$, which we suggest has quintet spin, where the reported BDE could be higher than the adiabatic BDE by the septet–quintet splitting of $Mn^+(H_2O)_2$, calculated by RB to be 4.4 kcal/mol. We predict that $Ti^+(H_2O)_4$ probably has doublet spin, but there is no information about the quartet–doublet splitting in $Ti^+(H_2O)_3$. RB did not consider the doublet states of $Ti^+(H_2O)_2$ so we cannot estimate errors in $\Delta H(3)$ if $Ti^+(H_2O)_3$ were doublet spin as well.

Conclusions

The bond energies of water molecules with first-row transition metal cations have been determined by collision-induced dissociation for up to four ligands. For metal ions studied in this work, the BDEs of the first and the second water are comparable, and the BDEs of the third and fourth ligands are lower than the first and second BDEs, except for Mn^+. Also, we confirm that the relative BDEs of the first and second ligand are correctly predicted by theory in all cases studied here within the cited errors.

(47) Sugar, J.; Corliss, C. *J. Phys. Chem. Ref. Data, Suppl. No. 2* **1985**, *14*, 1.

(48) Krishnamurthy, R.; Schaap, W. B. *J. Chem. Educ.* **1969**, *46*, 799.

The interplay between the binding of the ligand and the electronic state of the metal is seen to play an important role in the trends of BDEs as the number of ligands surrounding the ion is increased. In this work, we have the opportunity to systematically vary the number of electrons by varying the transition metal center. Our ability to maintain a constant charge on the ion, a constant number of ligands, and the same ligand across the first transition row isolates the effect of the number of electrons on the BDE.

We also conclude that to obtain accurate BDEs from CID studies, the experimental thresholds must be interpreted in light of the population of low-frequency vibrational modes, pressure effects in the data, and dissociation lifetimes. We find that determining bond energies from secondary ligand loss thresholds is less reliable and more difficult than interpreting the corresponding primary ligand loss threshold.

Acknowledgment. This work has been funded by the National Science Foundation, Grant No. CHE-9221241. The authors thank Dr. F. A. Khan and Professor T. G. Richmond for supplying us with $Mn(CO)_5COCF_3$ and Profs Michl and Squires for their comments.